https://doi.org/10.5194/egusphere-2022-1469
Preprint. Discussion started: 22 December 2022

An approach for projecting the timing of abrupt winter Arctic sea ice loss

Camille Hankel[1] and Eli Tziperman[1,2]

[1]Department of Earth and Planetary Sciences, Harvard University, 20 Oxford St, Cambridge, MA 02138
[2]School of Engineering and Applied Sciences, Harvard University

Correspondence: Camille Hankel (camille_hankel@g.harvard.edu)

Abstract. Abrupt and irreversible winter Arctic sea-ice loss may occur under anthropogenic warming due to the collapse of a sea-ice equilibrium at a threshold value of CO_2, commonly referred to as a tipping point. Previous work has been unable to conclusively identify whether a tipping point in Arctic sea ice exists because fully-coupled climate models are too computationally expensive to run to equilibrium for many CO_2 values. Here, we explore the deviation of sea ice from its equilibrium state under realistic rates of CO_2 increase to demonstrate how a few time-dependent CO_2 experiments can be used to predict the existence and timing of sea-ice tipping points without running the model to steady-state. This study highlights the inefficacy of using a single experiment with slow-changing CO_2 to discover changes in the sea-ice steady-state, and provides an alternate method that can be developed for the identification of tipping points in realistic climate models.

1 Introduction

The Arctic is warming at a rate at least twice as fast as the global mean with profound consequences for its sea ice cover. Summer sea ice is already exhibiting rapid retreat with warming (Nghiem et al., 2007; Stroeve et al., 2008; Notz and Stroeve, 2016), shortening the time that socioeconomic and ecological systems have to adapt. These concerns have motivated a large body of work dedicated to both observing present-day sea ice loss (Kwok and Untersteiner, 2011; Stroeve et al., 2012; Lindsay and Schweiger, 2015; Lavergne et al., 2019) and modeling sea ice to understand whether its projected loss is modulated by a threshold-like or "tipping point" behavior. Abrupt loss or a tipping point in Arctic sea ice could be driven by local positive feedback mechanisms (Curry et al., 1995; Abbot and Tziperman, 2008; Abbot et al., 2009; Kay et al., 2012; Leibowicz et al., 2012; Burt et al., 2016; Feldl et al., 2020; Hankel and Tziperman, 2021), remote feedback mechanisms that increase heat flux from the mid-latitudes (Holland et al., 2006; Park et al., 2015), or by the natural threshold corresponding to the seawater freezing point (Bathiany et al., 2016). Such a tipping point is mathematically understood as a change in the number or stability of steady-state solutions (Ghil and Childress, 1987; Strogatz, 1994) as a function of CO_2 and is also known as a "bifurcation". While most studies have concluded that there is no tipping point during the transition from perennial to seasonal ice cover (i.e., during the loss of *summer* sea ice), the existence of a tipping point during the loss of *winter* sea ice (transition to year-round ice-free conditions) continues to be debated in the literature (Eisenman, 2007; Eisenman and Wettlaufer, 2009; Notz, 2009; Eisenman, 2012), with three out of seven GCMs that lost their winter sea ice completely in the CMIP5 Extended RCP8.5

https://doi.org/10.5194/egusphere-2022-1469
Preprint. Discussion started: 22 December 2022

Scenario demonstrating an abrupt change that qualitatively looks like a tipping point, and *may* be related to a bifurcation (Hezel et al., 2014; Hankel and Tziperman, 2021). However, given the projected rapid changes to CO_2 in the coming centuries and the slower response of the climate system, we do not expect future sea ice to be fully equilibrated to the CO_2 forcing at a given time. Thus, we are interested in projecting the timing of abrupt winter Arctic sea ice changes under rapidly changing CO_2 forcing, when the standard steady-state tipping point analysis is not applicable.

Tipping points imply a bi-stability (meaning that sea ice can take on different values for the same CO_2 concentration), and hysteresis — an irreversible loss of sea ice even if CO_2 is later reduced. The computational efficiency of simple models allowed studies using them to calculate the region of winter sea-ice bi-stability by running simulations to steady-state at many different CO_2 values, which is not possible with expensive state-of-the-art Global Climate Models (GCMs). GCM studies therefore tend to use a single experiment with very gradual CO_2 increases and decreases (Li et al., 2013) or even a faster CO_2 change (Ridley et al., 2012; Armour et al., 2011), assuming such a run should approximate the behavior of the steady-state at different CO_2 concentrations. However, Li et al. (2013) further integrated two apparently bi-stable points and found that they equilibrated to the same value of winter sea ice: there was no "true" bi-stability at these two CO_2 concentrations. This calls into question the current use of time-changing CO_2 runs to study the bifurcation structure of sea ice.

In light of the difficulties in using model runs with time-changing CO_2 (hereafter "transient runs") for identifying tipping points, we identify a need to understand the relationship between these transient runs and the steady-state value of sea ice as a function of CO_2 in systems with and without bifurcations. Theoretical work (Haberman, 1979; Mandel and Erneux, 1987; Baer et al., 1989; Tredicce et al., 2004) and studies related to bi-stability in the Atlantic Meridional Overturning Circulation (Kim et al., 2021; An et al., 2021) have examined tipping points when the forcing parameter (CO_2 in our case) changes in time at a finite rate, and found that as the forcing parameter passes the bifurcation point, the system continues to follow the old equilibrium solution for some time before it rapidly transitions to the new one. This type of analysis has to our knowledge not yet been applied in the context of winter sea ice loss under time-changing CO_2 concentrations, nor compared in systems with and without a bifurcation.

In order to analyze how the hysteresis curve of sea ice under time-changing forcing relates to the steady-state behavior, we run a simple physics-based model of sea ice (Eisenman, 2007), configured in three different scenarios: with a large region of bi-stability, a small region of bi-stability, and no bi-stability in the equilibrium. These three scenarios span the range of possible behaviors of winter sea ice in state-of-the-art climate models. Each case is run with different rates of CO_2 increase (ramping rates). We use results from this model and from an even simpler 1D dynamical system to demonstrate that the convergence of the transient behavior (under time-changing forcing) to the equilibrium behavior is very slow as a function of the ramping rate of CO_2. In other words, even model runs with very slow-changing CO_2 forcing may simulate sea ice that is considerably out of equilibrium near the period of abrupt sea ice loss. Finally, we propose an approach for uncovering the underlying equilibrium behavior in comprehensive models where it is computationally inefficient to simulate steady-state conditions for many CO_2 values.

Some GCMs seem to exhibit a tipping point in winter sea ice, and others don't (Hezel et al., 2014; Hankel and Tziperman, 2021). The reasons are likely complex and involve numerous differences in parameters and parameterizations. It is not obvious

https://doi.org/10.5194/egusphere-2022-1469
Preprint. Discussion started: 22 December 2022

how to modify parameters in a single GCM to display all different behaviors. Therefore, we choose to use an idealized model of sea ice where we can directly produce different bifurcation behaviors to answer the question: is it possible to identify the CO_2 at which tipping points occur without running the model to a steady state for many CO_2 values? Answering such a question is an obvious prerequisite to tackling the problem of identifying climate bi-stability in noisy, high-dimensional, GCMs. In order to perform this analysis for each of the three scenarios mentioned above, we modify the strength of the albedo feedback via the choice of surface albedo parameters. The albedo values used here to generate the three scenarios are not meant to reflect realistic albedo values, but rather allow us to represent in a single model the range of sea ice equilibria behaviors that exist in different GCMs. We, therefore, follow in the footsteps of previous studies (e.g., Eisenman, 2007) that have also changed parameters (the latent heat of fusion) outside of their physically relevant regime in order to understand *summer* sea ice bifurcation behavior; here we follow the same approach to understand when a *winter* sea ice bifurcation can be detected without running an expensive climate model to steady-state.

2 Methods

2.1 Sea ice model

The Eisenman model contains four state variables: sea ice effective thickness (V, which is volume divided by the area of the model grid box), sea ice area (A), sea ice surface temperature (T_i), and mixed layer temperature (T_{ml}) for a single box representing the entire Arctic. The atmosphere is assumed to be in radiative equilibrium with the surface, and the model is forced with a seasonal cycle of insolation, of poleward heat transport, and of local optical thickness of the atmosphere, which represents cloudiness. The full equations of the sea ice model can be found in the original paper (Eisenman, 2007) and in the online Supporting Information; here, we highlight a few minor ways in which our implementation differs. First, for simplicity, we do not model leads, which in the original model were represented by capping the ice fraction at 0.95 rather than 1. Second, we use an approximation to the seasonal cycle of insolation (Hartmann, 2015) using a latitude of 75N. The atmospheric albedo is set to 0.425 to produce the same magnitude of the seasonal cycle as in the original model of Eisenman (2007).

2.2 Setup of simulations

In our transient-forcing scenarios (described below), we vary CO_2 in time which affects the mid-latitude temperature ($T_{\mathrm{mid-lat}}$) and the atmospheric optical depth (N) (see Supporting Information). Specifically, we increase the annual mean of $T_{\mathrm{mid-lat}}$ by 3 °C per CO_2 doubling and N by a ΔN that corresponds to 3.7 W/m^2 per doubling. All model parameters are as in (Eisenman, 2007) except as mentioned below.

We configure the model in three different scenarios that yield a wide CO_2 range of bi-stability in winter sea ice (Scenario 1), a small range of bi-stability in winter sea ice (Scenario 2), and no bi-stability in winter sea ice (Scenario 3). We do so by modifying the strength of the ice-albedo feedback by changing the albedos of bare ice (α_i), melt ponds (α_{mp}), and ocean (α_o), as listed in Table S1.

https://doi.org/10.5194/egusphere-2022-1469
Preprint. Discussion started: 22 December 2022

In each of the three scenarios, we tune the model (by adjusting the mean and amplitude of the atmospheric optical depth) to roughly match the observed seasonal cycle of ice thickness under pre-industrial CO_2 ($\sim$ 2.5–3.7 m, Eisenman, 2007). We then run each scenario with multiple CO_2 ramping rates (expressed in "years per doubling") with an initial stabilization period (fixed pre-industrial CO_2), a period of exponentially increasing CO_2 concentration (which corresponds to linearly increasing radiative forcing), another period of stabilization at the maximum CO_2, a period of decreasing CO_2, and a final period of stabilization at the minimum CO_2 value (see Supplemental Figure S2). Scenarios 2 and 3 are ramped to higher final CO_2 values than Scenario 1 so that they lose all their sea ice. We also directly calculate the steady-state behavior of the sea ice (as done in the original study) by running many simulations with fixed CO_2 values until the seasonal cycle of all the variables stabilizes. Because we expect multiple equilibria (which could be ice-free, seasonal ice, or perennial ice) at some CO_2 values in Scenarios 1 and 2, we run these steady-state simulations starting with both a cold (ice-covered) and a warm (ice-free) initial condition in order to find these different steady-states. In the ice-free initial condition runs, the ice-albedo feedback will still play an important role if the temperature cools sufficiently for ice to develop. At CO_2 values for which the sea ice is bistable, the ice-free initial condition evolves to a perennially ice-free steady-state, and the ice-covered initial condition evolves to a seasonally ice-covered steady-state (seen by the dotted and dashed lines respectively in Figs. 1a and 1c).

2.3 Cubic ODE

It turns out the main points we are trying to make about the transient versus equilibrium behavior of winter sea ice near a tipping point are not unique to the problem of winter sea ice, and in order to demonstrate this, we use the simplest mathematical model that can display tipping points. The cubic ODE used, while much simpler than the sea ice model above, has some of the key characteristics of the sea ice system (it is a non-autonomous system due to the time-depending forcing and has saddle-node bifurcations), which allows for direct comparison between the two models. The ODE equation,

$$\frac{dx}{dt} = -x^3 + \delta x + \beta(t), \qquad \beta(t) = \beta_0 + \mu t, \tag{1}$$

contains a time-changing forcing parameter, $\beta(t)$. We consider this differential equation in three scenarios, paralleling those used with the sea ice model: in Scenario 1, $\delta = 5$ leading to a wide region of bi-stability; in Scenario 2, $\delta = 1$ leading to a narrow region of bi-stability, and finally, in Scenario 3, $\delta = 0$ leading to a mono-stable system. The different values of δ, therefore, produce the same three scenarios that were achieved in the sea ice model by modifying the strength of the ice-albedo feedback. We mimic the hysteresis experiments of the sea ice model with a sequence of ramping up and ramping down (using different ramping rates, μ) with values of β ranging from -10 to 10 to sweep the parameter space that contains the bifurcations. We calculate the steady-states with fixed values of β ($\mu = 0$), starting with both a positive and a negative initial condition of x to yield two stable solutions when these exist.

We want to calculate the upper and lower CO_2 values of the hysteresis region in runs with time-changing (i.e., transient) CO_2 forcing. We do so by calculating the CO_2 value at which the March sea ice area drops below a critical threshold (50% ice coverage; results are insensitive to the specific value used) during increasing and decreasing CO_2 integrations: we denote these

https://doi.org/10.5194/egusphere-2022-1469
Preprint. Discussion started: 22 December 2022

CO_2 values CO_2^i and CO_2^d, respectively (see Supplemental Figure S9). The difference between CO_2^i and CO_2^d is referred to below as the "transient hysteresis width"; this width approaches the width of bi-stability at very slow ramping rates.

2.4 Predicting the CO_2 of the sea ice tipping point

In order to estimate the values of CO_2^i and CO_2^d that would have occurred for an infinitely slow ramping rate (in other words, the range of CO_2 for which there is bi-stability) without having to run a model to equilibrium for all values of CO_2 forcing, we fit a polynomial of the form $f(x) = mx^c + b$ to CO_2^i and CO_2^d as functions of the ramping rate x. Because c is negative, the fitted parameter b represents the prediction of CO_2^i and CO_2^d at infinitely slow ramping rates, i.e., in the steady state. We also calculate the uncertainty on the fitted parameter b by block-bootstrapping to account for auto-correlation; see Supporting Information. Other fits to CO_2^i and CO_2^d as a function of ramping rates, such as an exponential function $f(x) = a + b\exp(-cx)$ could in principle be used, although we found the fit to be less good in our case.

3 Results

In the following three subsections we discuss the behavior of the sea ice model and the cubic ODE under time-changing forcing, the relationship of the transient and equilibrium behaviors, and a method that we propose for inferring the existence and location of tipping points from the transient behavior.

3.1 Transient response of sea ice to time-changing CO_2

In Figs. 1b,d,f we plot the results of running all three scenarios (wide range of bi-stability (Scenario 1), narrow range of bi-stability (2), and no bi-stability (3)) under time-changing (transient) and fixed CO_2 values. In all scenarios, the experiments run with time-changing CO_2 exhibit transient hysteresis; the transient hysteresis width (lower horizontal gray bar in Fig. 1a) is larger for faster ramping rates (Figs. 1a,c,e). In Scenarios 1 and 2, whose equilibrium solutions (dashed and dotted black lines in Fig. 1) have a tipping point and therefore an infinite gradient of sea ice thickness vs. CO_2, the faster ramping rates also lead to more gradual (and finite) gradient of sea ice thickness vs. CO_2. The transient hysteresis loops across all scenarios at fast enough ramping rates (loops composed of the darkest blue and darkest red) are qualitatively similar in shape. This similarity indicates that from a single hysteresis run with time-changing CO_2 we cannot discern whether the underlying equilibrium behavior has a region of bi-stability or not, nor how wide the region of true bi-stability is. This result demonstrates that the apparent transient hysteresis loop found by Li et al. Li et al. (2013) could be due to a system with or without a true hysteresis (i.e. bi-stability in the steady-state behavior), consistent with their analysis.

The robustness and generality of the above results of the sea ice model are now demonstrated by showing that the simpler ODE (eqn. 1) produces the same behavior. The 1D ODE is also configured in three scenarios with wide bi-stability (Scenario 1), narrow bi-stability (Scenario 2), and no bi-stability (Scenario 3). In Figs. 1b,d,f we see transient hysteresis in all scenarios, similar to the result from the sea ice model. Specifically, even when there is only one stable equilibrium solution in both models (Scenario 3, panels e and f), there is still a narrow region of transient hysteresis. Thus, we find that the lack of distinction in

https://doi.org/10.5194/egusphere-2022-1469
Preprint. Discussion started: 22 December 2022

transient hysteresis loops between systems with and without bifurcations and the widening of the hysteresis loop with increased forcing parameter ramping rate appear to be robust results across these dynamical systems. Mathematically, this 1D system is fundamentally different from the sea ice model because it is not periodically forced. We show in the supplementary that adding a sinusoidal forcing term to the ODE does not qualitatively change our results.

3.2 Slow convergence of the transient hysteresis to the equilibrium behavior

As we saw in Fig. 1, the loss of sea ice with increasing CO_2 is very abrupt in the equilibrium (dashed and dotted black lines) and is infinite at the tipping point in Scenarios 1 and 2. On the other hand, the gradient is gradual and finite under time-changing forcing (blue and red curves), but steepens as the ramping rate decreases. We now quantify the rate of this steepening by examining the maximum gradient of sea ice loss during each transient simulation as a function of ramping rate (inverse of the years per doubling of CO_2). Our objective is to demonstrate that it is difficult to approach the equilibrium behavior using slower and slower-changing CO_2 runs (transient hysteresis experiments).

In Fig. 2a, we plot the maximum gradient of March sea ice thickness *with respect to* CO_2 during each hysteresis experiment, as a function of the CO_2 ramping rate. In Scenarios 1 and 2 (wide and narrow bi-stability respectively), the maximum gradient gets greater as the ramping rate is slower (Fig. 2a), consistent with Fig. 1 (e.g., steepening from dark blue to light blue curves in Figs. 1a,b). In particular, it approximately follows a negative power law as a function of ramping rate on both warming and cooling time series (dashed and solid lines in Fig. 2a). In Scenario 3, the maximum gradient is nearly insensitive to the ramping rate. In Fig. 2b, we see a similar result for the simple ODE, as seen by the shallowing of the power law from Scenarios 1 to 3 (though here the slope in Scenario 3 is clearly nonzero). Notably, the power law in the case with the largest region of bi-stability (Scenario 1) is approximately given by $\max(dx/d\beta) \propto \mu^{-1}$, where μ again is the ramping rate. A dependence of the maximum gradient on (ramping rate)$^{-1}$ in the case of wide bi-stability suggests that running a climate model with twice as gradual CO_2 ramping, leads to less than a factor of two increase in the gradient $\max(dV/d\mathrm{CO}_2)$. This is an important result because this implies that the distance between the CO_2 at the simulated transient "tipping point" and the CO_2 of the true (equilibrium) tipping point (which we want to estimate) only reduces by a factor of two. Thus, using more and more gradual ramping experiments may be an inefficient way to approach the equilibrium behavior of a physical system. The Supplementary Information further explains the above convergence rate of μ^{-1}.

3.3 Predicting the steady-state behavior of sea ice using only transient runs

One of our key results, presented next, is a method for finding the CO_2 concentration at which a bifurcation (if any) occurs in the equilibrium and estimating the associated hysteresis width using computationally feasible transient model runs. We are interested in this CO_2 concentration because it determines the threshold beyond which significant sea ice loss is practically irreversible Ritchie et al. (2021). In Fig. 3a, we plot a measure of the CO_2 values of the upper and lower edges of the transient hysteresis (by calculating the CO_2 at which the March sea ice area crosses a critical threshold, see Methods and Supplementary Figure S9). We plot this for the warming (increasing greenhouse concentration) trajectories in blue (CO_2^i) and for the cooling (decreasing greenhouse) trajectories in red (CO_2^d), as a function of the ramping rate for all three scenarios. As expected, as the

https://doi.org/10.5194/egusphere-2022-1469
Preprint. Discussion started: 22 December 2022

ramping rate gets slower CO_2^i and CO_2^d asymptote to the CO_2 values corresponding to the edges of bi-stability and the location of the true tipping points in the case of Scenarios 1 and 2 (denoted by the $\times$ symbols). In Scenario 3, CO_2^i and CO_2^d asymptote to the same value (transient hysteresis width approaches zero) because there is no bi-stability in the steady-state.

Finally, we demonstrate that fitting a curve to the edges of the transient hysteresis (CO_2^i and CO_2^d) as a function of the ramping rate can be used to predict CO_2^i and CO_2^d at infinitely slow ramping rates, and therefore to estimate the CO_2 value corresponding to a bifurcation in the equilibrium behavior without running a model to a steady-state. In Fig. 3a we plot CO_2^i and CO_2^d, and the curves that fit them (see Methods) as functions of the ramping rate, and the predicted values of CO_2^i and CO_2^d at infinitely slow ramping rates with a 95% confidence interval range shaded around them. We perform this fitting and estimation process using all the ramping experiments (18 different ramping rates total, as shown in Fig. 3a). We then repeat the fit using fewer and fewer experiments to explore how the uncertainty on predicted values of CO_2^i and CO_2^d increases as we move to only using a few fast ramping experiments that are more feasible when using full complexity climate models. Fig. 3b shows a summary of these analyses.

The predicted values of CO_2^i and CO_2^d are remarkably accurate for all scenarios (points approaching the red and blue $\times$ in Fig. 3b), even when excluding several of the slower ramping experiments. The uncertainties (indicated by the shaded blue and red bars around the points) in the predictions grow when excluding more experiments from the curve fitting process but still remain very low, especially for Scenarios 1 and 2. In predicting CO_2^d for Scenario 3, the uncertainties are a bit higher because the exponential form of our fit does not represent this case as well as the others, leading to serial correlation in the residuals. Finally, we can use the difference of the distributions CO_2^i and CO_2^d to calculate the probability that bi-stability– and thus a tipping point– exists (see Supplementary Information). Overall, these results demonstrate the potential for using several shorter runs with time-changing CO_2 forcing to estimate the CO_2 value of the tipping points and predict the existence of bi-stability in GCMs where equilibrium runs or long, slow-ramping hysteresis runs are computationally infeasible.

4 Discussion

We have shown that it is not feasible to use a single climate model run with time-changing (transient) forcing to estimate the true location of tipping points, the range of bi-stability in the steady-state, and even the existence of bi-stability at all, consistent with the findings of Li et al. (2013). We also showed that this seems to be a general issue in nonlinear systems, as the same problem occurs in a generic ODE undergoing transient hysteresis. Examining the maximum gradient of sea ice thickness with respect to CO_2 as a function of the ramping rate of CO_2, we find that very long model runs are needed to identify whether this value approaches infinity, which would indicate a bifurcation, and at what CO_2 this occurs. Instead, we propose using a few fast-ramping experiments to predict the true range of bi-stability and provide uncertainty estimates on this prediction. The ramping rates used here likely represent an upper bound for applying our method to GCMs (for example, in the context of the abrupt transition to a moist greenhouse (Popp et al., 2016), runaway greenhouse (Goldblatt et al., 2013), or snowball Earth state (Hyde et al., 2000)), as we expect GCMs to have longer equilibration timescales than the idealized Eisenman sea ice model.

https://doi.org/10.5194/egusphere-2022-1469
Preprint. Discussion started: 22 December 2022

We demonstrated that the method we propose can accurately predict the steady-state behavior of sea ice in a simple model; however, several challenges remain to deploying this method for use in full-complexity models. GCMs contain significant stochastic variability and multiple timescales of forcings that may render the calculated values of the diagnostics used here (such as the width of the transient hysteresis) uncertain. In addition, the functional form to fit to CO_2^i and CO_2^d in a GCM may require some further experimenting (such as trying an exponential rather than polynomial form) due to the more complex sea ice dynamics of the GCM. Nonetheless, we argue that using multiple runs to estimate the width of the bi-stability of a given climate variable and provide a quantified uncertainty on such a prediction offers a potential improvement over using a single hysteresis experiment. This approach still requires significant computational resources due to the need to run the model to equilibrium after the ramping up and ramping down of CO_2 in a hysteresis experiment.

Previous work has typically sought to identify bi-stability in sea ice because it would imply irreversibility of sea ice loss (in the sense that CO_2 would have to be reduced beyond the tipping point value to allow sea-ice re-growth). Here, we highlight a different perspective by focusing on realistic rates of CO_2 increase in addition to the steady-state behavior of sea ice. The SSP585 Scenario in CMIP6 corresponds to a ramping rate of approximately 60 years per CO_2 doubling: a rate at which sea ice in our idealized model already exhibits significant deviation from its steady state (60 years per doubling would fall between the 25 and 100 years per doubling blue curves in Figure 1, see also Fig. S2). Since we identify transient hysteresis in sea ice here in all scenarios even without a deep ocean and subsequent recalcitrant warming (Held et al., 2010), we expect transient hysteresis to be even more pronounced in GCMs and in the real climate when such long-timescale components are included. We therefore conclude that irreversibility *on policy-relevant timescales* is likely to occur in the real climate system regardless of whether an actual bifurcation (tipping point) in the equilibrium exists.

Code availability. An implementation of the Eisenman 2007 sea ice model in python used for this study can be found on Zenodo at: https://doi.org/10.5281/zenodo.6708812 (Hankel, 2022).

Author contributions. CH and ET designed the research project and prepared the manuscript together, CH implemented the model and conducted the experiments.

Competing interests. The authors declare no competing interests.

Acknowledgements. The authors would like to thank Ian Eisenman for his helpful input during the project and for the guidance in using his sea ice model. ET thanks the Weizmann Institute for its hospitality during parts of this work. This work has been funded by the NSF Climate Dynamics program (joint NSF/NERC) grant AGS-1924538.

https://doi.org/10.5194/egusphere-2022-1469
Preprint. Discussion started: 22 December 2022

References

Abbot, D. S. and Tziperman, E.: Sea ice, high-latitude convection, and equable climates, Geophysical Research Letters, 35, 2008.

Abbot, D. S., Walker, C., and Tziperman, E.: Can a convective cloud feedback help to eliminate winter sea ice at high CO_2 concentrations?, J. Climate, 22, 5719–5731, https://doi.org/10.1175/2009JCLI2854.1, 2009.

An, S.-I., Kim, H.-J., and Kim, S.-K.: Rate-Dependent Hysteresis of the Atlantic Meridional Overturning Circulation System and Its Asymmetric Loop, Geophysical Research Letters, 48, e2020GL090 132, 2021.

Armour, K., Eisenman, I., Blanchard-Wrigglesworth, E., McCusker, K., and Bitz, C.: The reversibility of sea ice loss in a state-of-the-art climate model, Geophysical Research Letters, 38, 2011.

Baer, S. M., Erneux, T., and Rinzel, J.: The slow passage through a Hopf bifurcation: delay, memory effects, and resonance, SIAM Journal on Applied mathematics, 49, 55–71, 1989.

Bathiany, S., Notz, D., Mauritsen, T., Raedel, G., and Brovkin, V.: On the potential for abrupt Arctic winter sea ice loss, Journal of Climate, 29, 2703–2719, 2016.

Burt, M. A., Randall, D. A., and Branson, M. D.: Dark warming, Journal of Climate, 29, 705–719, 2016.

Curry, J. A., Schramm, J. L., and Ebert, E. E.: Sea ice–albedo climate feedback mechanism, J. Climate, 8, 240–247, 1995.

Eisenman, I.: Arctic catastrophes in an idealized sea ice model, 2006 Program of Studies: Ice (Geophysical Fluid Dynamics Program), pp. 133–161, 2007.

Eisenman, I.: Factors controlling the bifurcation structure of sea ice retreat, Journal of Geophysical Research: Atmospheres, 117, 2012.

Eisenman, I. and Wettlaufer, J. S.: Nonlinear threshold behavior during the loss of Arctic sea ice, Proc Nat Acad Sci USA, 106, 28–32, 2009.

Feldl, N., Po-Chedley, S., Singh, H. K., Hay, S., and Kushner, P. J.: Sea ice and atmospheric circulation shape the high-latitude lapse rate feedback, npj Climate and Atmospheric Science, 3, 1–9, 2020.

Ghil, M. and Childress, S.: Topics in Geophysical Fluid Dynamics: Atmospheric Dynamics, Dynamo Theory and Climate Dynamics, Springer-Verlag, New York, 1987.

Goldblatt, C., Robinson, T. D., Zahnle, K. J., and Crisp, D.: Low simulated radiation limit for runaway greenhouse climates, Nature Geoscience, 6, 661–667, 2013.

Haberman, R.: Slowly varying jump and transition phenomena associated with algebraic bifurcation problems, SIAM Journal on Applied Mathematics, 37, 69–106, 1979.

Hankel, C.: camillehankel/sea_ice_thermo_0d: 0D-Sea-Ice-Model, https://doi.org/10.5281/zenodo.6708812, 2022.

Hankel, C. and Tziperman, E.: The Role of Atmospheric Feedbacks in Abrupt Winter Arctic Sea Ice Loss in Future Warming Scenarios, Journal of Climate, 34, 4435–4447, 2021.

Hartmann, D. L.: Global physical climatology, vol. 103, chap. Chapter 2, Newnes, 2015.

Held, I. M., Winton, M., Takahashi, K., Delworth, T., Zeng, F., and Vallis, G. K.: Probing the fast and slow components of global warming by returning abruptly to preindustrial forcing, Journal of Climate, 23, 2418–2427, 2010.

Hezel, P., Fichefet, T., and Massonnet, F.: Modeled Arctic sea ice evolution through 2300 in CMIP5 extended RCPs, The Cryosphere, 8, 1195–1204, 2014.

Holland, M. M., Bitz, C. M., and Tremblay, B.: Future abrupt reductions in the summer Arctic sea ice, Geophysical Research Letters, 33, 2006.

https://doi.org/10.5194/egusphere-2022-1469
Preprint. Discussion started: 22 December 2022

Hyde, W. T., Crowley, T. J., Baum, S. K., and Peltier, W. R.: Neoproterozoic 'snowball Earth' simulations with a coupled climate/ice-sheet model, Nature, 405, 425–429, 2000.

Kay, J. E., Holland, M. M., Bitz, C. M., Blanchard-Wrigglesworth, E., Gettelman, A., Conley, A., and Bailey, D.: The influence of local feedbacks and northward heat transport on the equilibrium Arctic climate response to increased greenhouse gas forcing, Journal of Climate, 25, 5433–5450, 2012.

Kim, H.-J., An, S.-I., Kim, S.-K., and Park, J.-H.: Feedback processes modulating the sensitivity of Atlantic thermohaline circulation to freshwater forcing timescales, Journal of Climate, 34, 5081–5092, 2021.

Kwok, R. and Untersteiner, N.: The thinning of Arctic sea ice, Phys. Today, 64, 36–41, 2011.

Lavergne, T., Sørensen, A. M., Kern, S., Tonboe, R., Notz, D., Aaboe, S., Bell, L., Dybkjær, G., Eastwood, S., Gabarro, C., et al.: Version 2 of the EUMETSAT OSI SAF and ESA CCI sea-ice concentration climate data records, The Cryosphere, 13, 49–78, 2019.

Leibowicz, B. D., Abbot, D. S., Emanuel, K. A., and Tziperman, E.: Correlation between present-day model simulation of Arctic cloud radiative forcing and sea ice consistent with positive winter convective cloud feedback, J. Adv. Model. Earth Syst., 4, https://doi.org/10.1029/2012MS000153, 2012.

Li, C., Notz, D., Tietsche, S., and Marotzke, J.: The transient versus the equilibrium response of sea ice to global warming, Journal of Climate, 26, 5624–5636, 2013.

Lindsay, R. and Schweiger, A.: Arctic sea ice thickness loss determined using subsurface, aircraft, and satellite observations, The Cryosphere, 9, 269–283, 2015.

Mandel, P. and Erneux, T.: The slow passage through a steady bifurcation: delay and memory effects, Journal of statistical physics, 48, 1059–1070, 1987.

Nghiem, S., Rigor, I., Perovich, D., Clemente-Colón, P., Weatherly, J., and Neumann, G.: Rapid reduction of Arctic perennial sea ice, Geophysical Research Letters, 34, 2007.

Notz, D.: The future of ice sheets and sea ice: Between reversible retreat and unstoppable loss, Proceedings of the National Academy of Sciences, 106, 20 590–20 595, 2009.

Notz, D. and Stroeve, J.: Observed Arctic sea-ice loss directly follows anthropogenic CO2 emission, Science, 354, 747–750, 2016.

Park, D.-S. R., Lee, S., and Feldstein, S. B.: Attribution of the recent winter sea ice decline over the Atlantic sector of the Arctic Ocean, Journal of Climate, 28, 4027–4033, 2015.

Popp, M., Schmidt, H., and Marotzke, J.: Transition to a moist greenhouse with CO2 and solar forcing, Nature communications, 7, 1–10, 2016.

Ridley, J., Lowe, J., and Hewitt, H.: How reversible is sea ice loss?, The Cryosphere, 6, 193, 2012.

Ritchie, P. D., Clarke, J. J., Cox, P. M., and Huntingford, C.: Overshooting tipping point thresholds in a changing climate, Nature, 592, 517–523, 2021.

Stroeve, J., Serreze, M., Drobot, S., Gearheard, S., Holland, M., Maslanik, J., Meier, W., and Scambos, T.: Arctic sea ice extent plummets in 2007, Eos, Transactions American Geophysical Union, 89, 13–14, 2008.

Stroeve, J. C., Serreze, M. C., Holland, M. M., Kay, J. E., Malanik, J., and Barrett, A. P.: The Arctic's rapidly shrinking sea ice cover: a research synthesis, Climatic change, 110, 1005–1027, 2012.

Strogatz, S.: Nonlinear dynamics and chaos, Westview Press, 1994.

Tredicce, J. R., Lippi, G. L., Mandel, P., Charasse, B., Chevalier, A., and Picqué, B.: Critical slowing down at a bifurcation, American Journal of Physics, 72, 799–809, 2004.

https://doi.org/10.5194/egusphere-2022-1469
Preprint. Discussion started: 22 December 2022

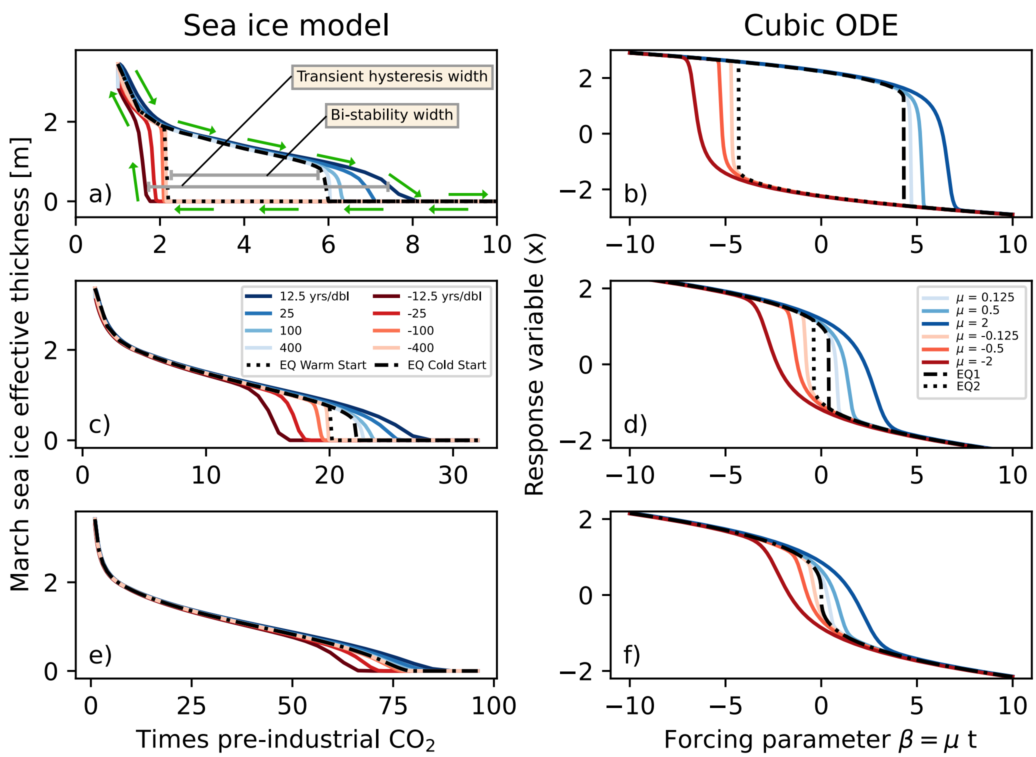

Figure 1. Transient hysteresis runs (time-changing forcing) and equilibrium runs (fixed forcing) for average March sea ice effective thickness (sea ice volume divided by area of the grid cell; panels a,c,d) and the simple ODE from Eq. 1 (b,d,f). The first row corresponds to Scenario 1 (wide bi-stability), the second row to Scenario 2 (narrow bi-stability), and the third to Scenario 3 (no bi-stability). Blue lines indicate simulations with increasing forcing (CO_2 or β), while red lines indicate simulations with decreasing forcing. Dashed and dotted black lines indicate the steady-state values of sea ice or the ODE variable x. These two black lines are different when the two initial conditions evolve to two different steady-states. The legends indicate the different ramping rates (represented by darker colors for faster rates), which are in units of years per CO_2 doubling in the case of the sea ice model. The green arrows demonstrate the direction of evolving sea ice effective thickness during the transient hysteresis experiments.

https://doi.org/10.5194/egusphere-2022-1469
Preprint. Discussion started: 22 December 2022

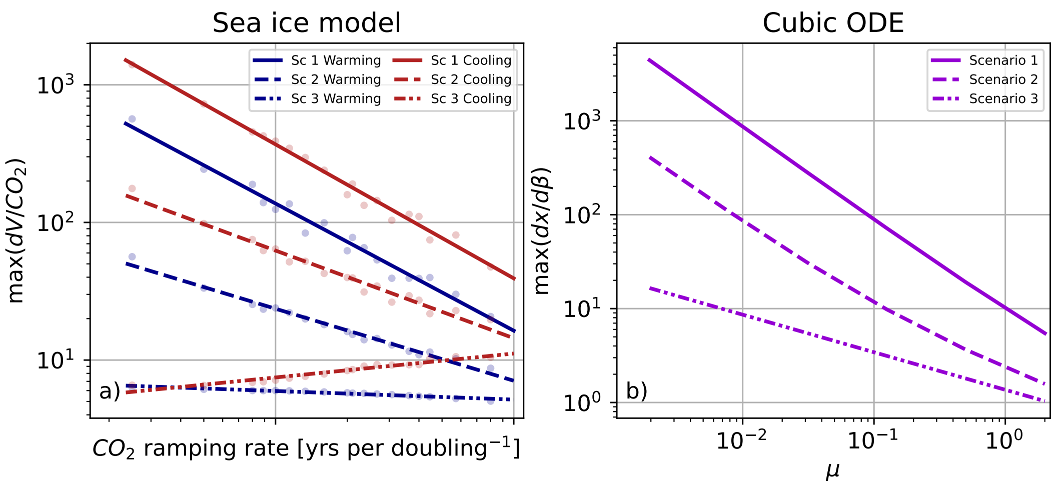

Figure 2. Maximum gradient of sea ice effective thickness with respect to CO_2 in panel a, and the maximum gradient of x with respect to the forcing parameter β in panel b during transient simulations. For the sea ice model (a) the data points from the 18 different runs are shown as faded points, with a superimposed line of best fit. For the cubic ODE (b) the maximum gradient lines corresponding to increasing and decreasing forcing time series are identical due to the symmetry around $\beta = 0$ seen in Fig. 1b, d, and f.

https://doi.org/10.5194/egusphere-2022-1469
Preprint. Discussion started: 22 December 2022

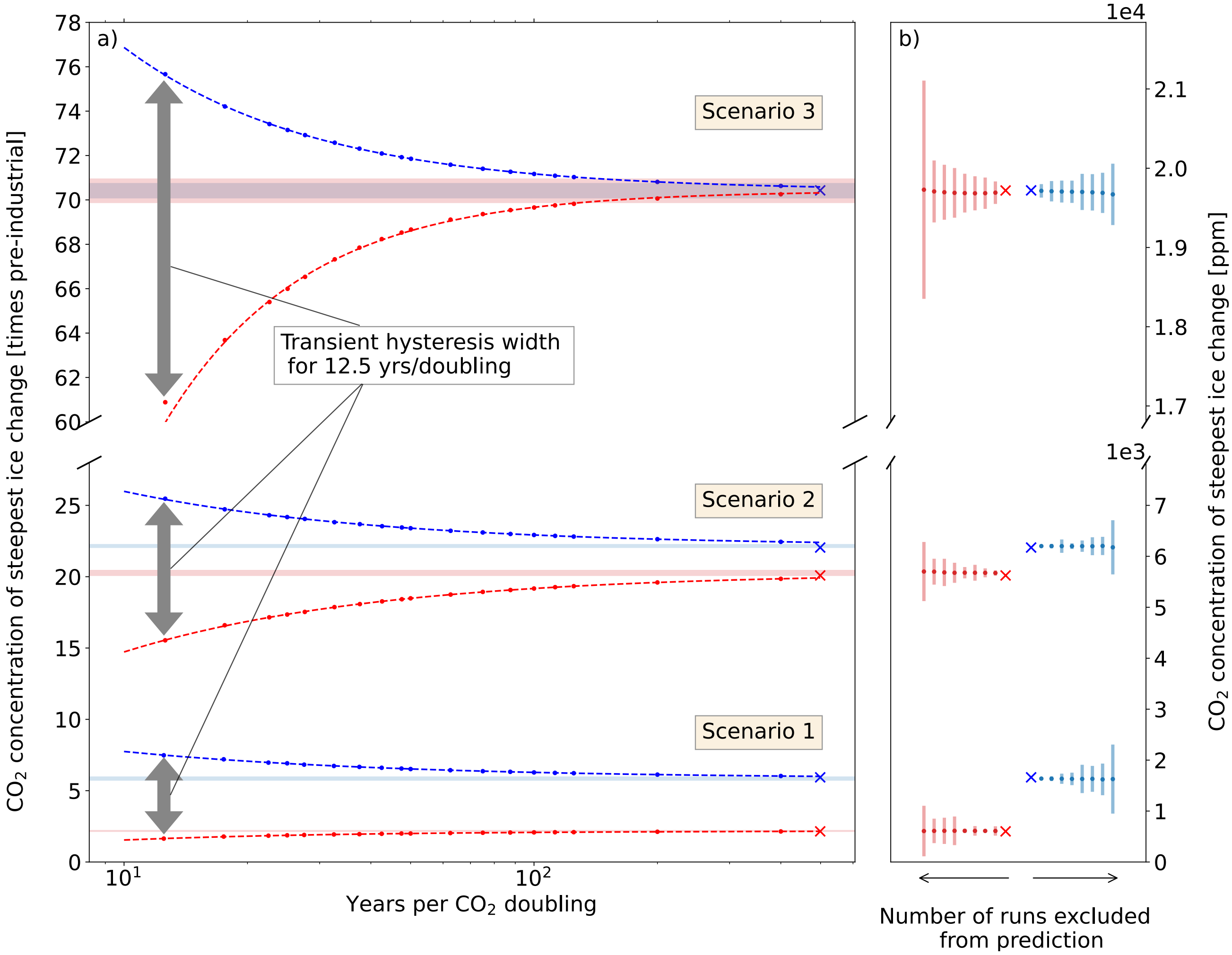

Figure 3. Estimating the equilibrium tipping point value from the transient hysteresis runs. In panel a, the scatter points show the CO_2 value of the right and left edges of the transient hysteresis (CO_2^i and CO_2^d, located along increasing (blue) and decreasing (red) CO_2 time-series respectively) for different ramping rates. The dashed lines show the curve that is fitted to the scatter points, and the shaded blue and red bands show $\pm 2\sigma$ around the predicted values of CO_2^i and CO_2^d at infinitely slow ramping rates. The blue and red $\times$'s show the true equilibrium values of CO_2^i and CO_2^d (calculated from the fixed CO_2 runs starting with cold and warm initial conditions respectively). In panel b, we analyze the accuracy of this prediction as we use fewer transient runs. For the three scenarios, we show the result of sequentially excluding the most gradual ramping simulations from the curve-fitting process used for predictions. The dots and the corresponding bars represent the predicted equilibrium values of CO_2^i and CO_2^d, and $\pm 2\sigma$ around the prediction, and dots moving away from the true value with larger error bars correspond to excluding more and more runs from the calculation.